*Ecological Applications*, 27(5), 2017, pp. 1498–1513


# Evaluating a new method for reconstructing forest conditions from General Land Office survey records

Carrie R. Levine,[1,9] Charles V. Cogbill,[2] Brandon M. Collins,[3] Andrew J. Larson,[4] James A. Lutz,[5] Malcolm P. North,[6] Christina M. Restaino,[7] Hugh D. Safford,[7,8] Scott L. Stephens,[1] and John J. Battles[1]

[1]*Department of Environmental Science, Policy, and Management, University of California, 130 Mulford Hall, Berkeley, California 94720 USA*
[2]*Harvard Forest, Harvard University, 324 North Main Street, Petersham, Massachusetts 01366 USA*
[3]*University of California Center for Fire Research and Outreach, College of Natural Resources, University of California, Berkeley, California 94720 USA*
[4]*Department of Forest Management, University of Montana, 32 Campus Drive, Missoula, Montana 59812 USA*
[5]*S. J. & Jessie E. Quinney College of Natural Resources, Utah State University, 5230 Old Main Hill, Logan, Utah 84322 USA*
[6]*USDA Forest Service, Pacific Southwest Research Station, 1731 Research Park Drive, Davis, California 95618 USA*
[7]*Department of Environmental Science and Policy, University of California, Davis, One Shields Avenue, Davis, California 95616 USA*
[8]*USDA Forest Service, Pacific Southwest Region, 1323 Club Drive, Vallejo, California 94592 USA*

*Abstract.* Historical forest conditions are often used to inform contemporary management goals because historical forests are considered to be resilient to ecological disturbances. The General Land Office (GLO) surveys of the late 19th and early 20th centuries provide regionally quasi-contiguous data sets of historical forests across much of the Western United States. Multiple methods exist for estimating tree density from point-based sampling such as the GLO surveys, including distance-based and area-based approaches. Area-based approaches have been applied in California mixed-conifer forests but their estimates have not been validated. To assess the accuracy and precision of plotless density estimators with potential for application to GLO data in this region, we imposed a GLO sampling scheme on six mapped forest stands of known densities (159–784 trees/ha) in the Sierra Nevada in California, USA, and Baja California Norte, Mexico. We compared three distance-based plotless density estimators (Cottam, Pollard, and Morisita) as well as two Voronoi area (VA) estimators, the Delince and mean harmonic Voronoi density (MHVD), to the true densities. We simulated sampling schemes of increasing intensity to assess sampling error. The relative error (RE) of density estimates for the GLO sampling scheme ranged from 0.36 to 4.78. The least biased estimate of tree density in every stand was obtained with the Morisita estimator and the most biased was obtained with the MHVD estimator. The MHVD estimates of tree density were 1.2–3.8 times larger than the true densities and performed best in stands subject to fire exclusion for 100 yr. The Delince approach obtained accurate estimates of density, implying that the Voronoi approach is theoretically sound but that its application in the MHVD was flawed. The misapplication was attributed to two causes: (1) the use of a crown scaling factor that does not correct for the number of trees sampled and (2) the persistent underestimate of the true VA due to a weak relationship between tree size and VA. The magnitude of differences between true densities and MHVD estimates suggest caution in using results based on the MHVD to inform management and restoration practices in the conifer forests of the American West.

*Key words:* *California; density; forest; plotless density estimator; Voronoi area.*

## Introduction

Forests in the western United States are threatened by a suite of stressors that include altered fire regimes, legacy effects from timber harvesting, a warming climate, chronic air pollution, and uncharacteristically severe attacks by insects and pathogens (Perry et al. 2011, Bytnerowicz et al. 2013, Hessburg et al. 2016). In response, management seeks to restore diverse landscapes that maintain native species and characteristic processes (North et al. 2009, Hessburg et al. 2016, Stephens et al. 2016). These management goals are informed by the structure and composition of the forest prior to European settlement (Churchill et al. 2013), a time when western forests are thought to have sustained form and function despite fire, drought, and insect attack (Mast et al. 1999, Stephens et al. 2015). Given the current emphasis on forest restoration and resilience in public lands (USFS 2011, 2013) accurate characterizations of historical forests are particularly important.

Estimates of pre-settlement forest conditions are derived from data with inherent limitations. Historical inventories are a primary source of information (Stephens 2000, Hagmann et al. 2013) but even the most

Manuscript received 3 October 2016; revised 10 January 2017; accepted 22 February 2017. Corresponding Editor: Carolyn H. Sieg.
[9] E-mail: crlevine@berkeley.edu

geographically extensive records (e.g., >10,000 ha; Stephens et al. 2015) may not necessarily represent regional forest characteristics. Forest reconstructions using fire scars, stumps, and tree rings also provide useful references (Taylor 2004, North et al. 2007) but physical evidence of the pre-settlement forest degrades with time and the effort involved constrains the spatial extent of the reconstruction. In contrast, the public land survey system conducted by the General Land Office (GLO) is a systematic, historical sample of trees over a broad domain from Ohio to the West Coast of the United States (Schulte and Mladenoff 2001).

The purpose of the GLO survey was to delineate boundaries of federal lands for sale. The survey consisted of 9.7 × 9.7 km (6 × 6 mile) townships containing 36 1.6 × 1.6 km (1 × 1 mile) sections. Section corners marked with permanent monuments demarcated the end of 1.6-km section lines and quarter corners were located equidistant to two section corners. In order to provide reference points to the corners, nearby bearing trees (also called witness trees) were selected. Section corners were referenced with four bearing trees; quarter corners were referenced with two bearing trees. For each bearing tree, the distance and direction from the point along with species identification and stem diameter were recorded. In effect, these bearing tree records represent a systematic sample of forest conditions (Schulte and Mladenoff 2001).

While the GLO bearing tree data overcome the restricted geographic extent shared by historical inventories and forest reconstructions, it is a sparse sample (i.e., 1 point per 0.8 km) beset by questions regarding data quality and analysis (Bourdo 1956, Bouldin 2008, Hanberry et al. 2011, Liu et al. 2011). Cottam (1949) was one of the first to use the pre-settlement survey to estimate past forest characteristics. As he noted, the key challenge is an accurate estimate of tree density from the information contained in the bearing trees. Although surveyor bias and error in the selection of bearing trees are concerns (Bourdo 1956, Grimm 1984, Bouldin 2008, Liu et al. 2011, Williams and Baker 2011), this paper focuses on the fundamental task of calculating tree density from distance data (e.g., Cottam and Curtis 1956, Morisita 1957, Pollard 1971, Williams and Baker 2011). Specifically, we evaluated the performance of a new plotless density estimator (PDE) developed to maximize the utility of GLO data to reconstruct pre-settlement forests in the arid western US by using area-based metrics (sensu Williams and Baker 2011, Baker 2014) as opposed to traditional distance-based estimators.

### *Background*

Plotless density estimators (PDEs) are a frequent alternative to plot-based sampling for forest inventory (Kronenfeld 2009). They rely on point-to-tree and/or tree-to-tree distances to efficiently sample heterogeneous landscapes. Of the many possible PDEs (e.g., Engeman et al. 1994), we tested the bias and precision of three PDEs that have been applied by previous studies to GLO data. These PDEs are appropriate to GLO data because they rely only on the distance data recorded by surveyors when documenting bearing trees. We refer to these PDEs by the name of their most often-cited source: Cottam, Pollard, and Morisita (Table 1). The equations share a similar format to estimate tree density from a sample of points where the distance to the nearest tree is measured in each sector (four 90° sectors for corner points; two 180° sectors for quarter corners). This common format for tree density (λ) includes a unit scalar ($K$), an expression of design parameters (Ω), and an estimate of either the squared mean or the mean squared point-to-tree distance (ptd)

Table 1. Equations used to estimate tree density (trees/ha) in this study.

| Name | Equation | Source |
|---|---|---|
| Cottam (C) | $\lambda_C = K \frac{m}{4} \frac{1}{\left(\sum_{j=1}^{n}\sum_{i=1}^{m}\frac{r_{ij}}{nm}\right)^2}$ | 1 |
| Pollard (P) | $\lambda_P = K \frac{(mn-1)m}{\pi} \frac{1}{\sum_{j=1}^{n}\sum_{i=1}^{m} r_{ij}^2}$ | 2 |
| Morisita (M) | $\lambda_M = K \frac{(m-1)m}{\pi n} \sum_{j=1}^{n} \frac{1}{\sum_{i=1}^{m} r_{ij}^2}$ | 3 |
| Delince (D) | $\lambda_D = K \frac{1}{mn/\sum_{i=1}^{mn}\frac{1}{VA(tree_i)}}$ | 4 |
| Mean Harmonic Voronoi Density (MHVD) | $\lambda_{MHVD} = K \frac{1}{mn/\sum_{i=1}^{mn}\frac{1}{MVA(tree_i)}}$ | 5 |

*Notes:* Term definitions are $m$, number of sectors; $n$, number of points; $r_{ij}$, the distance from point $j$ to tree $i$; $K$, the scaling coefficient to return density in trees/ha; λ, tree density; VA, the measured Voronoi area; MVA, the mean Voronoi area (estimated). In this paper, $r_{ij}$ is measured in meters, thus $K$ = 10,000. Also note that, in all cases, only the nearest tree in each sector is measured. Thus the total number of trees is $m \times n$ ($mn$).

*Sources:* 1, Cottam and Curtis (1956); 2, Pollard (1971: Eq. 6); 3, Morisita (1957: Eq. 31); 4, Delince (1986: Eq. 7); 5, Williams and Baker (2011: Table 2).

$$\lambda \propto K \quad \Omega \quad \frac{1}{\overline{\text{ptd}^2} \text{ or } (\overline{\text{ptd}})^2} \tag{1}$$

Applications of the Cottam estimator to GLO survey data include Rhemtulla et al. (2009) and Maxwell et al. (2014), the Pollard-Kronenfeld and Wang (2007), the Morisita-Hanberry et al. (2012).

The theoretical basis for these three PDEs rests on the assumption that the distribution of the point-to-tree distances indicates the average surface area occupied by the average tree (Cottam and Curtis 1956, Morisita 1957). Cottam and Curtis (1956) consider this sample space as the exclusive surface area occupied by the nearest trees. Thus the reciprocal of the average area occupied (area per tree) is the density (trees per area). However point-to-tree distances are unbiased variables only when the spatial distribution of trees follows a random pattern and the density of trees remains constant (Klein and Vilcko 2006). The PDEs vary in their performance, but in general accuracy and precision decrease as the trees diverge from random spacing and/or tree density varies across the landscape (Cottam and Curtis 1956, Engeman et al. 1994, Kronenfeld 2009). The challenge posed by a non-random distribution of trees is particularly important in dry forests of western North America, where clumped tree spacing is typical (Larson and Churchill 2012).

The new PDE recommended by Williams and Baker (2011) uses the predicted Voronoi area (VA) of individual trees to overcome the limitations of distance-based estimators. VAs are applied in a variety of disciplines to describe spatial positions of points on a plane (Okabe et al. 2000). Mark and Esler (1970) were among the first to suggest a design-based, point-to-tree PDE that relied on the exclusion zone of individual trees to avoid potential biases introduced by the point pattern of the trees. This zone delineates a polygon where the tree defining the polygon will be the closest to any sample point in the polygon. Delince (1986) subsequently provided the theoretical justification for this approach and the application to calculate tree density from point samples (Table 1). In Delince's (1986) method, the exclusion zone is the VA with the vertices of the VA defined by half the distance to each neighboring tree. The obvious constraint with the Delince PDE with regard to the GLO data is that only the distance to the nearest tree in each sector is recorded at the corner points. There is no information on the location of the neighboring trees in GLO data.

The innovation in Williams and Baker (2011) was the adaptation of Delince's (1986) approach to the GLO data. Since there was no way to measure the VA of bearing trees in historical data sets such as the GLO data, they developed region-specific regression equations from contemporary data that predict VA as a function of tree diameter and local tree density, which can then be applied to historical data (Table 1). The accuracy of the VA prediction is crucial. The expectation that tree size is a good indicator of VA assumes that competition is a major factor driving the spatial arrangement of trees. In short, bigger trees are expected to have larger exclusion zones. A host of distance-dependent tree competition indices incorporate tree size to account for this size-dependency (Biging and Dobbertin 1992, Aakala et al. 2013) but competition is not only distance-dependent (Lorimer 1983). For mixed-conifer forests in the Sierra Nevada, Biging and Dobbertin (1995) reported that distance-independent competition indices performed slightly better than the best distance-dependent measures. The assumption inherent in Williams and Baker's (2011) methodology that the size of a tree is the most important determinant of its spatial configuration relative to neighboring trees must be investigated in order to determine whether the density estimates derived from this approach are accurate.

### *Research objectives*

The application of this new area-based PDE to GLO data from dry conifer forests across the western US has often produced drastically higher estimates of pre-settlement tree density than expected (Baker 2012, 2014, Williams and Baker 2012). For example, in the Californian mixed-conifer forests on the western slopes of the Sierra Nevada, pre-settlement tree density estimates based on Baker's (2014) analysis of GLO data exceeded estimates based on historic forest inventories by 200–500% (Stephens et al. 2015). Hagmann et al. (2013, 2014) found similar discrepancies between the historical forest inventories they analyzed in mixed-conifer forests of central and northern Oregon and density estimates for the same areas reported by Baker (2012) using the new area-based PDE. These results challenge our understanding of the natural dynamics of the Sierra Nevada and eastern Oregon mixed-conifer forests where frequent low- and moderate-severity fires were thought to maintain relatively open forests (Hessburg et al. 2015; Safford and Stevens 2017). Moreover, Baker's (2014) reconstructions raised important questions regarding the appropriate strategy to restore contemporary Sierra Nevada forests (Odion et al. 2014, Hanson and Odion 2016).

This new perspective on the historical western forest has engendered criticism (e.g., Hagmann et al. 2013, Baker 2014, Fule et al. 2014, Williams and Baker 2014) but the performance of the novel density estimator that underpins these controversial findings has not been independently tested. Therefore, we simulated a GLO sampling scheme in six 4-ha mapped stands that span much of the latitudinal range of mixed-conifer forest in the California Floristic Province, some of which had experienced fire exclusion whereas others had relatively intact fire regimes. Mapped stands, where the location of all trees is known, are required to verify the true VA of trees. We compared the accuracy of traditional PDEs to the method used by Baker (2014) and assessed whether VA regression equations are able to accurately predict true VA. Given the potential of the GLO bearing tree

data to characterize pre-settlement forest conditions of the United States, it is essential to review the theoretical basis of any new PDE and to test its application.

## Methods

### *Study sites*

We identified six old-growth mixed-conifer and pine-dominated stands across the latitudinal gradient of the Sierra Nevada and Sierra de San Pedro Martir of California, USA and Baja California, Mexico (Table 2). Sites included three stands on the western slope of the Sierra Nevada: one stand in the Plumas National Forest (PLUM), one stand in the Teakettle Experimental Forest (TEAK), and one stand in Yosemite National Park (YOSE). A fourth site (BRID) was located on the eastern slope of the Sierra Nevada in the Humboldt-Toiyabe National Forest. All of the California stands had not been harvested but experienced approximately 100 yr of fire exclusion. The remaining two stands were in the Sierra de San Pedro Martir National Park on the western slope of the Sierra de San Pedro Martir, where fire suppression did not begin until the 1970s (Stephens et al. 2010). The two sites in Baja differ in their underlying geology, with one site on soil derived from metamorphic parent material (META) and the other site on soil derived from granitic parent material (GRAN; Stephens and Gill 2005, Fry et al. 2014). In addition to covering a latitudinal gradient of the mixed-conifer and pine forests, these stands also encompass a density gradient ranging from 159 to 784 trees/ha (Table 2). Each stand included in this study was 4 ha in area and included the mapped locations of all stems ≥9.5 cm diameter at breast height (DBH; 1.37 m; Fig. 1). Five of the stands were 200 × 200 m in configuration and the PLUM stand was 100 × 400 m. To illustrate the range of results, we included figures from two sites: YOSE, a site that is representative of contemporary density in the Sierra Nevada (FIA 2015), and GRAN, a site that is representative of pre-settlement density (Stephens et al. 2015). Figures for the other four sites can be found in Appendix S1.

### *Site-specific spatial patterns*

We applied an inhomogeneous Ripley's $L$ function ($L$) to determine the spatial patterning of the trees at each of the six stands. The inhomogeneous function avoids assuming a null model characterized by a homogeneous Poisson process, which may result in the misinterpretation of the point structure when point density varies within a mapped study area (Wiegand and Moloney 2004). We used a radius of 25 m at the PLUM stand (the maximum allowable radius due to the stand configuration) and a radius of 30 m at the other five stands. Thirty meters was chosen as the cutoff because this radius was larger than the maximum distance required to locate a nearest neighbor to a random sampling point in the least dense stand (GRAN, 28 m maximum distance to nearest neighbor). Thus, a 30-m radius captures all potential tree-to-tree competitive interactions relevant to PDE calculations. For each stand, we simulated 1000 runs of a random distribution of trees to determine the 95% confidence interval (CI). The empirical $L$ value from the mapped trees was compared to the simulated 95% CI to determine at what scales the distribution of trees significantly differed from a random distribution (Cressie 2015). The criterion for significance was the non-overlap of observed $L$ with the 95% CI of the random simulations.

### *GLO density estimators*

We compared density estimates from the six mapped stands based on the three traditional PDEs (i.e., the Cottam, Pollard, and Morisita) as well as the mean-based harmonic Voronoi density (MHVD, Table 1). Williams and Baker (2011) found the MHVD to be one of the most accurate Voronoi-based estimators they tested, and Baker (2014) applied the MHVD to sites in the Sierra Nevada of California. The calculation of the traditional PDEs relies on the information contained in the GLO survey, namely the number of corners ($n$), the number of sectors ($m$), and the point-to-tree distances ($r$) in each sector (Table 1). In contrast, the MHVD requires predicting the mean Voronoi area (MVA) via a three-step process: (1) predict a tree's crown radius (CR) from the

Table 2. Site description for the six stands included in this study. Density and basal area are for trees ≥9.5 cm DBH.

| Site | Latitude (W) | Longitude (N) | Elevation (m) | Density (trees/ha) | Basal area ($m^2$/ha) | Fir (%) | Pine (%) | Source |
|---|---|---|---|---|---|---|---|---|
| PLUM | 121°02′ | 39°55′ | 1158–1219 | 784 | 87 | 87 | 3 | 1 |
| YOSE | 119°49′ | 37°46′ | 1774–1911 | 562 | 56 | 79 | 13 | 2 |
| TEAK | 119°02′ | 36°58′ | 1880–2485 | 313 | 56 | 64 | 27 | 3 |
| META | 115°59′ | 31°37′ | 2400–2500 | 254 | 23 | 0 | 100 | 4 |
| BRID | 119°28′ | 38°24′ | 2500–2600 | 236 | 36 | 38 | 50 | 4 |
| GRAN | 115°59′ | 31°37′ | 2400–2500 | 159 | 25 | 13 | 87 | 4 |

*Notes:* Sites are PLUM, Plumas National Forest; YOSE, Yosemite National Park; TEAK, Teakettle Experimental Forest; META, the site in the Sierra de San Pedro Martir with soil derived from metamorphic parent material; BRID, Humboldt-Toiyabe National Forest near Bridgeport, California, USA; GRAN, the site in the Sierra de San Pedro Martir with soil derived from granitic parent material. Fir and pine refer to the percentage of the number of trees in either category in each 4-ha stand.
*Sources:* 1, Levine et al. (2016); 2, Lutz et al. (2012); 3, North et al. (2007); 4, Fry et al. (2014).

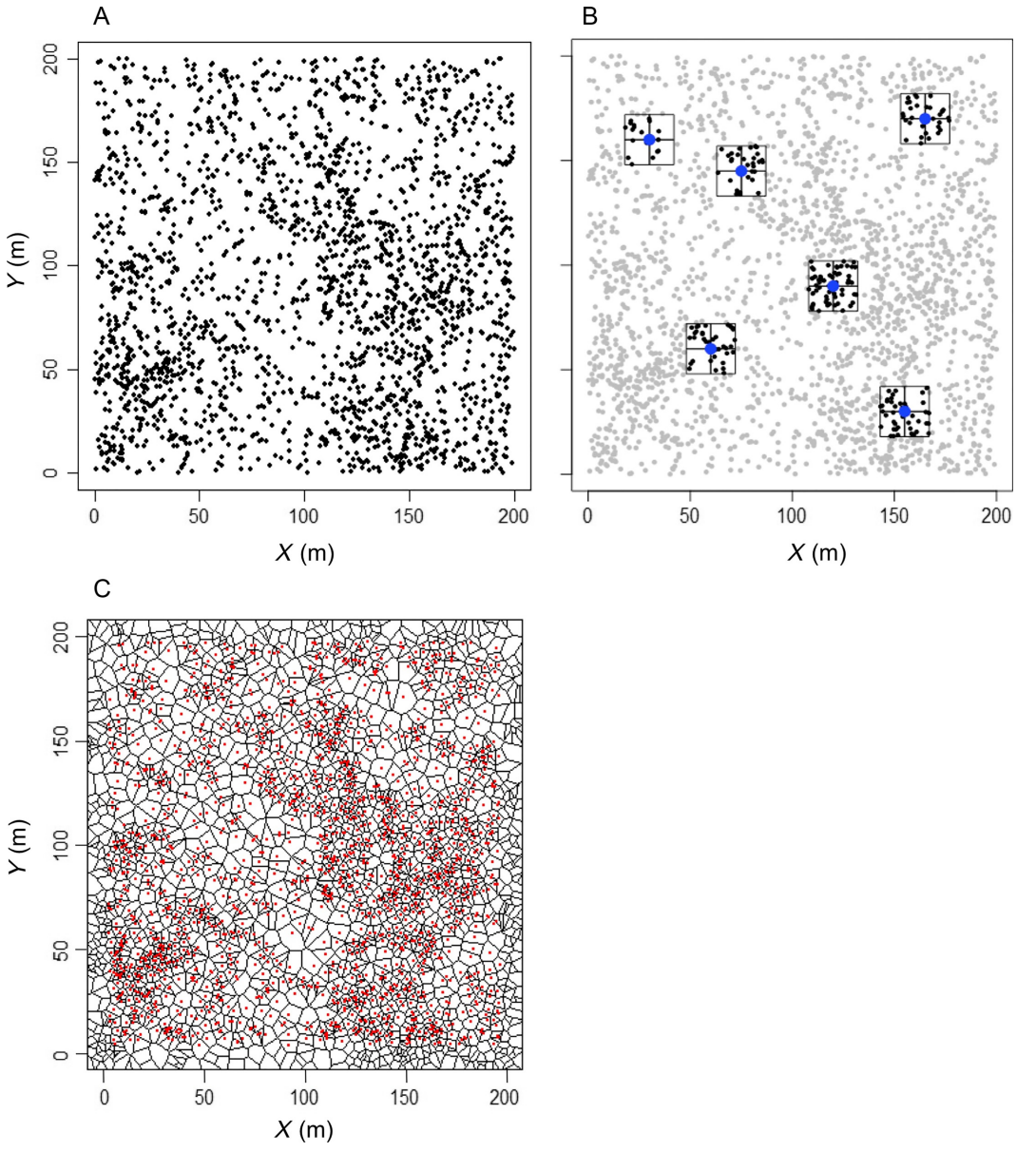


FIG. 1. An example from Yosemite National Park (YOSE) of the mapped tree plots used in the analysis. (A) The spatial distribution of trees in the mapped plot, (B) section corner sampling points (blue) and neighboring trees for a six-point sampling scheme, (C) and true Voronoi areas. [Color figure can be viewed at wileyonlinelibrary.com]

allometric relationship between crown size and stem diameter; (2) calculate the mean neighborhood density (MND) correction factor; and (3) estimate a tree's MVA from its CR scaled by the MND (Williams and Baker 2011). The CR for tree$_i$ was predicted from the diameter at breast height (DBH, at a height of 1.37 m) of tree$_i$ according to the equation

$$\ln(\mathrm{CR}) = a + b \quad \ln(\mathrm{DBH}) \tag{2}$$

where $a$ and $b$ are species-specific regression parameters for CR (Table D1 in Baker 2014). At each corner, the MND was calculated as

$$\mathrm{MND}_j = \frac{1}{\sum_{i=1}^{m} \frac{r_{ij}}{m}^2} \tag{3}$$

where $r$ is the distance from the sampling point$_j$ to the nearest neighbor tree$_i$ in $m$ sectors (Williams and Baker 2011). The MVA of tree$_i$ at sampling point$_j$ was then estimated as

$$\mathrm{MVA}(\mathrm{tree}_i) = \exp \quad a + b \quad \frac{\ln[\mathrm{CR}(\mathrm{tree}_i)}{\mathrm{MND}_j} \tag{4}$$

where $a$ and $b$ are species-specific regression parameters for MVA (Table D1 in Baker 2014), MND$_j$ from Eq. 3,

and CR(tree$_i$) from Eq. 2. Note that we used DBH to estimate CR in accord with the equation in Baker (2014). However, an unpublished erratum (W. Baker, *personal communication*) corrected the CR predictor to diameter at stump height (DSH; 0.30 m). Thus we also calculated MHVD with DSH. See Appendix S2 for details.

### *Bias and precision assessment*

We applied simulations to quantify the performance of the PDEs. Each test included 1000 realizations of randomly placed sampling corners in each of the six mapped stands. Sample corner intensity spanned the range of GLO point pools considered by Williams and Baker (2011)—3, 6, 9, and 21—as well as the recommended minimum intensity of 50 points (Kronenfeld 2009, Hanberry et al. 2011) and a saturation intensity of 1000 points. To minimize edge effects, the location of the random points was excluded from a buffer zone along the stand boundaries with the buffer width ranging from 10 to 20 m depending on tree density. Less dense stands required a larger buffer to ensure the presence of a bearing tree in each sector for every simulated point.

The GLO sampling regime includes section corners with four bearing trees (one tree in each 90° quadrant) and quarter corners with two bearing trees (one tree in each 180° semicircle). Bearing trees are referred to as nearest neighbors (nn) for the purposes of density calculation. When calculating the PDEs, we treated all corners as either sections corners with four bearing trees (4 nn) or quarter corners with two bearing trees (2 nn). We did not apply the correction factors developed in Williams and Baker (2011) to allow the mixing of results from section corners and quarter corners. While the correction factors increase the number of trees available from the GLO data because both 4 nn and 2 nn corners can be included, the use of the weights has to our knowledge only been vetted for the Cottam (Cottam and Curtis 1956). Moreover, it is clear from both theory and practice that the number of neighbors measured greatly affects the estimate (Morisita 1957, Engeman et al. 1994, Kronenfeld 2009). For example, Kronenfeld (2009) demonstrated for the Pollard that the bias in the estimated density diminishes as nn increases, ultimately approaching an asymptote near the true density as nn approaches 50. By excluding correction factors, our comparisons avoided a potential confounding factor.

Although not appropriate for GLO data because it requires measuring the VA, we included the Delince PDE in the simulation because it constitutes the theoretical underpinning of the MHVD approach. Its inclusion can help to deduce the source of any bias observed. To compute the Delince (Table 1), the nearest bearing tree to each point (1 nn) was selected and its true VA was calculated from the mapped trees.

Results from the 1000 realizations were summarized by the median as the measure of central tendency and the 95% CI as the measure of variation. Bias was defined by the relative error (RE)

$$\mathrm{RE} = \frac{\lambda_{\mathrm{sim}}}{\lambda_{\mathrm{true}}} \tag{5}$$

where $\lambda_{\mathrm{sim}}$ is the median density from the 1000 realizations and $\lambda_{\mathrm{true}}$ is the true density of the mapped stand. RE < 1 implies underestimates; RE > 1 implies overestimates. Precision was defined by the relative root mean square error (rRMSE)

$$\mathrm{rRMSE} = \frac{\mathrm{RMSE}_{\mathrm{sim}}}{\lambda_{\mathrm{true}}} \tag{6}$$

where $\mathrm{RMSE}_{\mathrm{sim}}$ is the root mean square error of the 1000 realizations in each simulation and $\lambda_{\mathrm{true}}$ is the true density of the mapped stand. Larger values of rRMSE imply less precision.

### *MHVD deconstruction*

We evaluated the three steps needed to calculate the MHVD. For crown radius (CR, Eq. 2), we compared the regression fits described in Baker (2014) to equations estimated from Forest Health Monitoring (FHM) data collected as part of the Forest Inventory and Analysis Program. This database included measured crown radii from monitoring plots in the mixed-conifer forest of the Sierra Nevada in California (*available online*).[10] Predictions of CR were fit from the FHM data for all species present in the six stands (10 species total; *n* per species ranging from 59 to 746).

Williams and Baker (2011) used the mean neighborhood density (MND, Eq. 3) to adjust the MVA prediction by the local density, with the assumption that a tree of a given diameter will have a larger MVA in a less dense stand and a smaller MVA in a more crowded stand. To isolate the effect of the MND correction, we simulated a six-point section corner (4 nn) and a six-point quarter corner (2 nn) sampling scheme in each of the six mapped stands and reported the median MND and 95% CI (from 1000 realizations) for the 2-nn and 4-nn sampling schemes. This six-point scheme is recommended by Williams and Baker (2011) as being sufficient for estimating density with a 22% relative mean absolute error (RMSE). We used the 1000 simulated MND values to estimate the median and 95% CI of the MVA for a representative tree (Eq. 4). For each stand, the representative tree was defined by the dominant species and the median DBH; MVA was fit using the equation parameters in Baker (2014).

We tested the strength of the relationship between CR/MND and true VA by least-squares regression. We calculated the MVA regression parameters in Eq. 4 for the common species (>5% dominance) in each stand and compared them to the species-specific fits in Baker

[10] http://www.fia.fs.fed.us/tools-data/other_data/index.php

(2014). Only section corners (4 nn) were considered for the MND values in this analysis to avoid potential confounding errors from calculating MND with two or four bearing trees. CR was estimated using parameters derived from the FHM data set (as above); MND was calculated for 21 regularly spaced section corners (4 nn). True VAs were calculated from mapped tree locations. Thus in this analysis we had large, well-distributed samples for both the CR and MVA regressions.

We assessed the accuracy of the MVA regression equation by comparing the predicted VA of individual trees to the true VA. We used the tree maps to calculate the true VA of each tree. For each stand, a buffer ranging from 5 to 18 m from the stand boundaries was applied with the width set to ensure that trees included in the analysis had a neighbor on all sides. MND was derived from 21 regularly spaced section corners (4 nn, as above). Only section corners were considered in this analysis to avoid potential confounding errors from calculating MND with two or four bearing trees. The MVA for trees was computed using the CR and MVA coefficients in Baker (2014); the recorded tree species and DBH; and the MND for the point nearest to each tree (Eq. 4). We also estimated the mean difference ($\overline{\text{VA}}_{\text{difference}}$) between MVA and true VA, calculated as

$$\overline{\text{VA}}_{\text{difference}} = \sum_{i=1}^{n} \frac{\text{MVA}_i \quad \text{VA}_{\text{true}_i}}{n} \tag{7}$$

where $i$ refers to the individual tree and $n$ is the total number of trees. We calculated the comparison for each stand with three different size classes of trees: trees ≥9.5 cm DBH, trees >20 cm DBH, and trees >60 cm DBH. All data processing and analyses were conducted in R version 3.2.4 (R Development Core Team 2014); spatial metrics relied on functions in the spatstat package (Baddeley et al. 2015).

## Results

### *Tree spatial distribution in each stand*

Despite differences in geography, density, and composition, the overall spatial pattern was consistent among all six stands. Trees were significantly clumped at spatial scales relevant to the PDE calculation and showed inhibition at larger scales due to the presence of gaps throughout the stand (Appendix S1: Fig. S1). The inhomogeneous Ripley's $L$ values exceeded the 95% CI for randomly spaced trees from 0 to 1 m at the minimum and 13–29 m at the maximum: an indication of an aggregated distribution (Appendix S1: Fig. S1).

### *Bias and precision assessment*

Considering only the GLO-appropriate PDEs for a 50-point sampling intensity, the least biased estimate of tree density in every stand was obtained with the Morisita and the most biased was obtained with the MHVD (Table 3). The direction of the bias in the Morisita varied with some underestimates and some overestimates. In contrast, the Cottam and Pollard consistently underestimated true density and the MHVD always overestimated true density. In general, the 4 nn sampling had less bias than the 2-nn sampling. This difference was particularly pronounced in the MHVD. For the 2-nn MHVD, the median REs ranged from 2.04 to 3.58 whereas, for the 4 nn MHVD, it ranged from 1.16 to 1.59 (Table 3). The performance of the Delince PDE was exceptional (Table 3). The biases were small and non-directional with median REs ranging from 0.92 to 1.14. The performance in regard to the bias of individual estimators documented for the 50-point sampling intensity was consistent at other sampling intensities (Appendix S1: Tables S1–S9).

The precision of the tree density estimates systematically increased with sampling intensity for all PDEs. Not only did the width of confidence interval shrink with increasing point density (Fig. 2; Appendix S1: Fig. S2 for the Delince) but the rRMSE also declined systematically with increasing point density in every case (Appendix S1: Tables S1–S9). Moreover, the 4-nn sampling scheme consistently produced more precise estimates (i.e., lower rRMSE) than the 2 nn.

Among the PDEs, the MHVD was the least precise for a given sampling scheme and intensity (Fig. 2, Table 3). The Morisita tended to produce less precise density estimates at sample intensities <50. The improvement in precision with increasing sample intensity was steepest for the MHVD and Delince. For both PDEs, the rRMSE was an order of magnitude lower for the 1000-point sample compared to the three-point sample (Appendix S1: Tables S1–S9). In the 50-point sampling simulations, the Delince obtained not only the least biased estimates of density but also the most precise (Table 3). The Morisita 4-nn estimator was the next best in terms of minimizing bias and maximizing precision.

### *MHVD deconstruction*

Tree diameter proved to be a robust predictor of crown radius. Based on the coefficient of determination ($r^2$), the fits of ln(CR) to ln(DBH) for conifer trees in the FHM data ranged from 0.43 for *Pseudotsuga menziesii* (PSME, $n$ = 196) to 0.83 for *Pinus monticola* (PIMO, $n$ = 59). The $r^2$ values for the hardwoods were lower, ranging from 0.22 for *Populus tremuloides* (POTR, $n$ = 65) to 0.44 for *Quercus kelloggii* (QUKE, $n$ = 254). All fits showed a significantly increasing relationship of ln(CR) to ln(DBH) ($P < 0.05$; Appendix S1: Fig. S3). The slope and intercepts of the relationship of ln(CR) to ln(DBH) were generally similar to those listed in Baker (2014) for the same species.

The 4 nn sampling scheme resulted in a significantly higher mean distance to nearest trees compared to the

TABLE 3. Relative performance of the density estimates for the 50-point simulations.

| Site | PLUM | YOSE | TEAK | META | BRID | GRAN |
|---|---|---|---|---|---|---|
| True density (trees/ha) | 784 | 562 | 313 | 254 | 236 | 159 |
| Cottam (four trees) | | | | | | |
| 2.5% CI | **0.79** | 0.66 | 0.49 | 0.52 | 0.63 | 0.68 |
| Median | **0.93** | 0.79 | 0.62 | 0.66 | 0.75 | 0.80 |
| 97.5% CI | **1.09** | 0.96 | 0.82 | 0.85 | 0.91 | 0.97 |
| rRMSE | **0.10** | 0.22 | 0.38 | 0.36 | 0.26 | 0.22 |
| Cottam (two trees) | | | | | | |
| 2.5% CI | **0.74** | **0.62** | 0.47 | 0.49 | 0.57 | **0.66** |
| Median | **0.92** | **0.80** | 0.63 | 0.66 | 0.73 | **0.83** |
| 97.5% CI | **1.16** | **1.05** | 0.87 | 0.89 | 0.94 | **1.08** |
| rRMSE | **0.13** | **0.22** | 0.37 | 0.36 | 0.29 | **0.20** |
| Pollard (four trees) | | | | | | |
| 2.5% CI | **0.79** | 0.64 | 0.43 | 0.46 | 0.62 | 0.66 |
| Median | **0.92** | 0.75 | 0.54 | 0.58 | 0.73 | 0.77 |
| 97.5% CI | **1.07** | 0.90 | 0.69 | 0.74 | 0.87 | 0.92 |
| rRMSE | **0.11** | 0.26 | 0.46 | 0.43 | 0.29 | 0.25 |
| Pollard (two trees) | | | | | | |
| 2.5% CI | **0.72** | 0.59 | 0.41 | 0.43 | 0.55 | **0.64** |
| Median | **0.90** | 0.76 | 0.54 | 0.58 | 0.68 | **0.80** |
| 97.5% CI | **1.11** | 0.98 | 0.73 | 0.79 | 0.88 | **1.04** |
| rRMSE | **0.15** | 0.25 | 0.46 | 0.44 | 0.33 | **0.22** |
| Morisita (four trees) | | | | | | |
| 2.5% CI | **0.80** | **0.72** | **0.71** | **0.67** | **0.69** | **0.69** |
| Median | **0.96** | **0.94** | **1.15** | **1.06** | **0.89** | **0.87** |
| 97.5% CI | **1.21** | **1.24** | **2.08** | **1.76** | **1.23** | **1.29** |
| rRMSE | **0.11** | **0.14** | **0.40** | **0.30** | **0.17** | **0.20** |
| Morisita (two trees) | | | | | | |
| 2.5% CI | **0.66** | **0.61** | **0.65** | **0.67** | **0.57** | **0.62** |
| Median | **0.92** | **0.90** | **1.24** | **1.19** | **0.85** | **0.94** |
| 97.5% CI | **1.57** | **1.62** | **2.85** | **2.78** | **1.70** | **1.98** |
| rRMSE | **0.25** | **0.31** | **0.78** | **0.67** | **0.38** | **0.37** |
| MHVD (four trees) | | | | | | |
| 2.5% CI | 1.02 | 1.16 | 1.15 | **0.94** | 1.09 | **0.99** |
| Median | 1.16 | 1.40 | 1.59 | **1.30** | 1.34 | **1.21** |
| 97.5% CI | 1.32 | 1.72 | 2.31 | **1.80** | 1.69 | **1.50** |
| rRMSE | 0.18 | 0.16 | 0.14 | **0.38** | 0.37 | **0.25** |
| MHVD (two trees) | | | | | | |
| 2.5% CI | 1.72 | 2.17 | 2.30 | 2.08 | 2.13 | 2.03 |
| Median | 2.04 | 2.89 | 3.58 | 3.09 | 2.83 | 2.68 |
| 97.5% CI | 2.47 | 4.17 | 6.13 | 4.70 | 3.84 | 3.72 |
| rRMSE | 1.06 | 1.07 | 1.02 | 2.25 | 1.89 | 1.75 |
| Delince (one tree) | | | | | | |
| 2.5% CI | **0.83** | **0.79** | **0.77** | **0.72** | **0.71** | **0.73** |
| Median | **0.99** | **0.99** | **1.14** | **1.02** | **0.92** | **0.96** |
| 97.5% CI | **1.21** | **1.27** | **1.85** | **1.59** | **1.21** | **1.41** |
| rRMSE | **0.10** | **0.12** | **0.34** | **0.24** | **0.14** | **0.18** |

*Notes:* Results are reported as relative values with the results from the 1000 realizations divided by the true density. rRMSE refers to the relative root mean square error. Boldface text indicates site estimates where the 95% CI of the simulation overlaps the true density.

2 nn sampling (Fig. 3A, C). This difference translated into a lower MND. When we applied the MND to the estimation of the MVA of a representative tree, the 4 nn MND correction resulted in significantly higher estimations of MVA for the same tree relative to the 2 nn MND (Fig. 3B, D). The results were replicated at every site—the 2 nn sampling resulted in a higher MVA estimate (Appendix S1: Fig. S4).

For the mapped trees in the six stands we tested, CR was a very weak predictor of VA (Fig. 4). Although the slope of the regression line was positive and often significant (i.e., $P < 0.05$), the fits were very poor. The

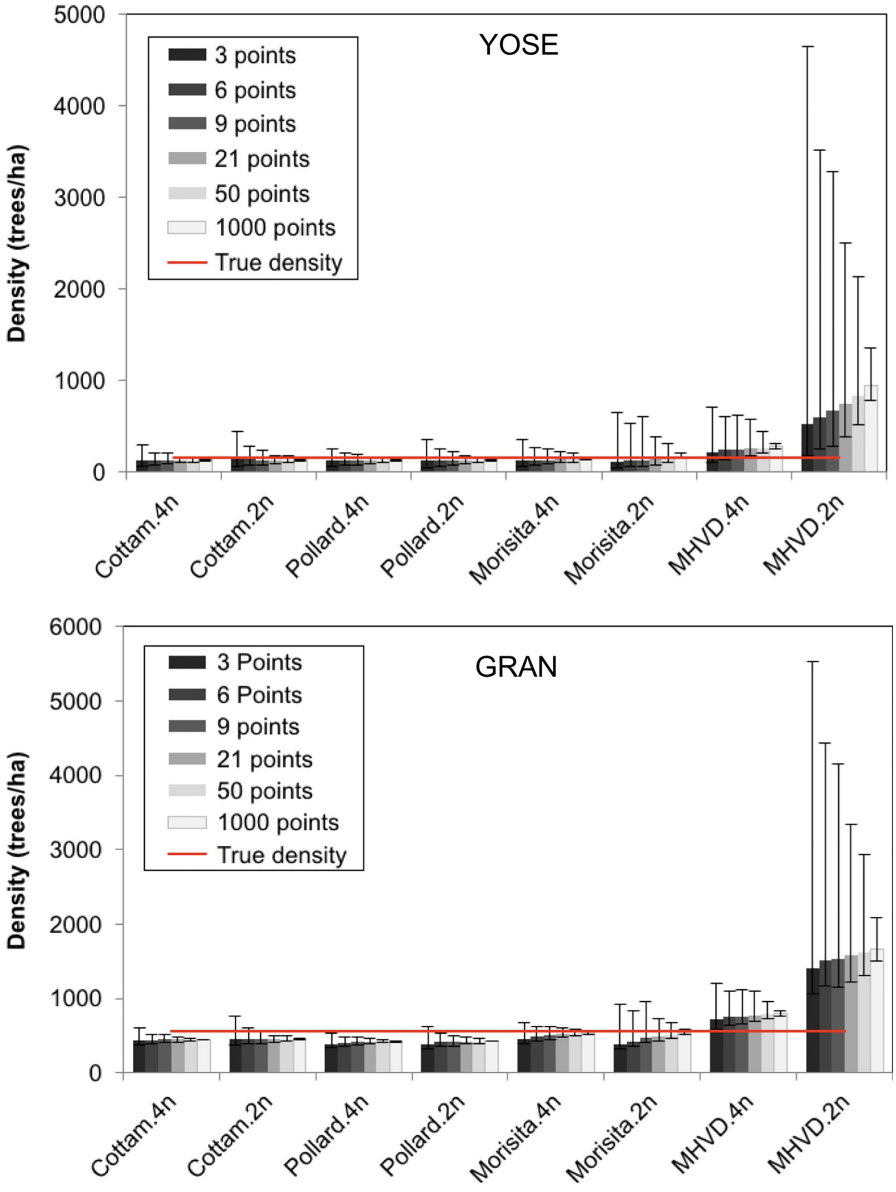


FIG. 2. Results of simulations testing the effect of sampling intensity (number of sampled points) on the Cottam, Pollard, Morisita, and MHVD estimators at the YOSE and GRAN (developed from granitic material) sites. Bars show the median value of 1000 realizations and error bars show the 95% confidence intervals. Simulation summaries can be found in Appendix S1: Tables S1–S9. [Color figure can be viewed at wileyonlinelibrary.com]

coefficient of determination ($r^2$) ranged from a minimum of 0.003 for *Abies concolor* (ABCO) at the GRAN site ($n$ = 73) to a maximum 0.29 for *Pinus jeffreyi* (PIJE) at the META site ($n$ = 773; Appendix S1: Table S10).

The MVA calculated with the parameters provided in Baker (2014) consistently underestimated the true VA of the trees at all sites (Fig. 5; Appendix S1: Fig. S5). The difference increased with increasing tree size (Table 4). For example, the median $VA_{difference}$ for all mapped trees (DBH ≥ 9.5 cm) in the six stands was 21.2 $m^2$; for large trees (DBH > 60 cm) the median difference was 36.7 $m^2$. The underestimate of MVA relative to the true VA increased as tree density decreased (Table 4).

Calculating MVA using DSH as opposed to DBH reduced the bias of the MHVD 4 nn estimator. However, both the MHVD 2 nn and 4 nn estimators overestimated stand density in all cases. Additionally, MVA consistently underestimated true VA, regardless of whether MVA was calculated with DSH or DBH. Results for relevant analyses using DSH in place of DBH are presented in Appendix S2.

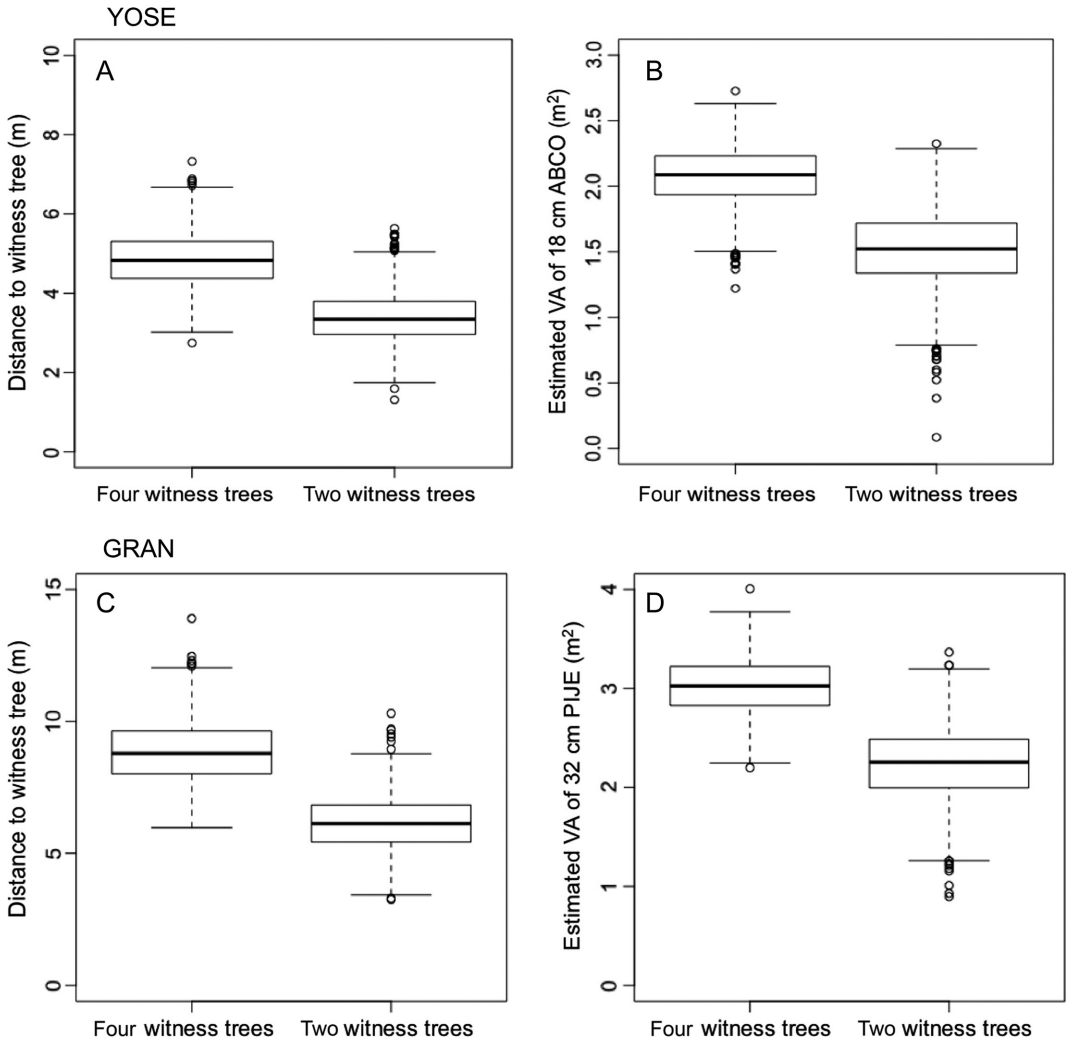


FIG. 3. Simulation results (1000 runs) of the mean neighborhood distance (A, C) when two witness trees or four witness trees are used for a six-point sampling scheme for the YOSE and GRAN sites, respectively. The discrepancy in mean neighborhood distance is reflected in the estimate of the Voronoi area of a single tree of the dominant species (B, D) of the median DBH in that plot using the method and equation parameters in Baker (2014). Results for other sites are shown in Appendix S1: Fig. S4. ABCO refers to *Abies concolor* (white fir); PIJE refers to *Pinus jeffreyi* (Jeffrey pine). The midline of the boxplot represents the median of the data, the upper and lower limits of the box represent the third and first quartile of the data, and the whiskers represent 1.5× the interquartile range from the third and first quartile. The points represent data outside 1.5× the interquartile range from the third and first quantile.

## DISCUSSION

The mean harmonic Voronoi area (MHVD) as specified in Baker (2014) consistently provided the least accurate estimate of tree density among the plotless density estimators (PDE) tested. In every scenario, the MHVD was biased toward overestimating tree density with lower precision than alternative metrics. Two factors contributed to this bias: (1) the difference in mean neighborhood distance (MND) between 2 nn and 4 nn sampling and (2) the persistent underestimate of the true Voronoi area (VA).

Williams and Baker (2011) recognized that local tree density influences the allometric relationship between tree diameter and crown radius, specifically that for a given species and DBH, the crown width decreases with increasing tree density (Bragg 2001). They evaluated three different crown scaling factors and found that the MND was ultimately the best. Baker (2014) subsequently applied this MND to scale CR in the Sierra Nevada based on the recommendation of Williams and Baker (2011) and supported by local validation (Appendix D in Baker 2014). The well-known influence of the number of sectors in the CR scaling factor (e.g., Cottam and Curtis 1956) was clearly a concern; one of the alternative neighborhood density equations Williams and Baker (2011) tested explicitly included a correction for mean distances obtained with 2-nn vs. 4-nn sampling (the correction factor neighborhood density, CFND, Table 2 in Williams and Baker 2011). However, the PDE

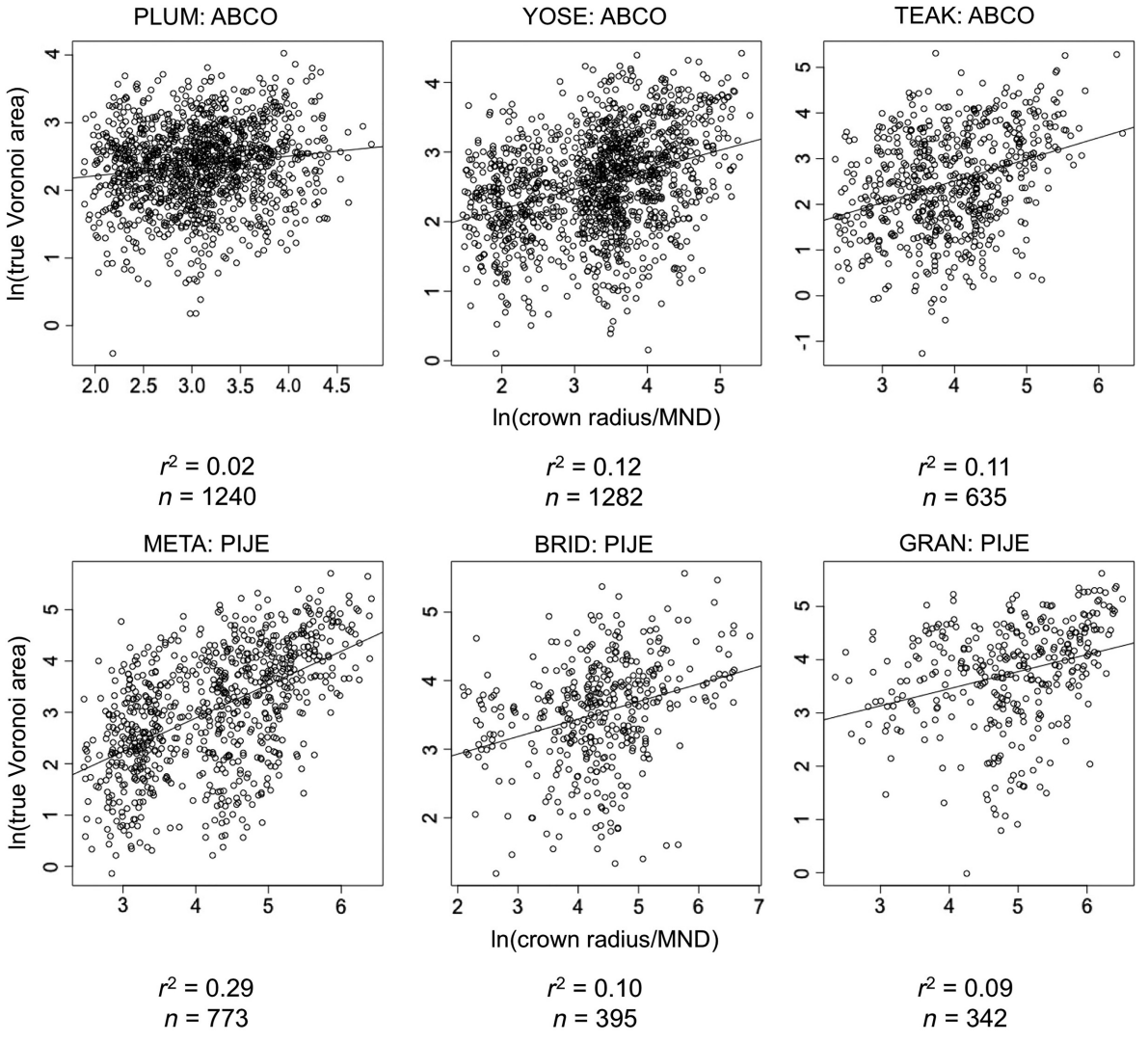


FIG. 4. The relationship of true Voronoi area (VA) to crown radius (CR) for the dominant tree species at each of the six study sites. The crown radius was estimated using parameters for species-specific fits derived from Forest Health Monitoring measurements in Sierra Nevada mixed-conifer plots (PIJE, $n = 164$; ABCO, $n = 746$). MND is the mean neighborhood distance (see Eq. 3). ABCO refers to *Abies concolor* (white fir); PIJE refers to *Pinus jeffreyi* (Jeffrey pine).

that included the CFND (the correction factor geometric Voronoi estimator, CFGVD) was generally not as accurate as the MHVD in their evaluation (Table 3 in Williams and Baker 2011). In contrast, in our simulations the lack of a correction factor for the number of bearing trees included in the calculation of MHVD almost doubled (1.85×), on average, the estimate of tree density in the 2 nn sampling compared to the 4 nn (Appendix S1: Tables S7 and S8). Why this flaw was not noted earlier may be due to two facts. Baker (2014) developed local MVA regressions as functions of CR and MND (Baker 2014, Appendix D) but only used points with four bearing trees. In addition, the performance of the MHVD in the Sierra Nevada was not compared to plot estimates of tree density as done in previous applications (e.g., Baker 2012, Williams and Baker 2012).

Independent of the MND, the MVA equations in Baker (2014) systematically underestimated true VA (Fig. 5, Table 4). In particular, the MVA (calculated using a MND based on 4 nn) reached a maximum area much lower than the true VA. For example, at YOSE, the median true VA was 18 $m^2$ while the median MVA was only 8 $m^2$, and 18% of the mapped trees had a true VA that exceeded the maximum MVA (Fig. 4). Similar results were obtained at the five other stands and the effect appeared to increase as density decreased (Appendix S1: Fig. S5). One explanation for the mismatch could be that samples included in Baker's (2014) MVA regressions did not capture the full range of variation.

We found a weak predictive ability of CR in our stands, with the $r^2$ of true ln(VA)~ln(CR/MND) for conifers ranging from 0.003 to 0.29 (Appendix S1:

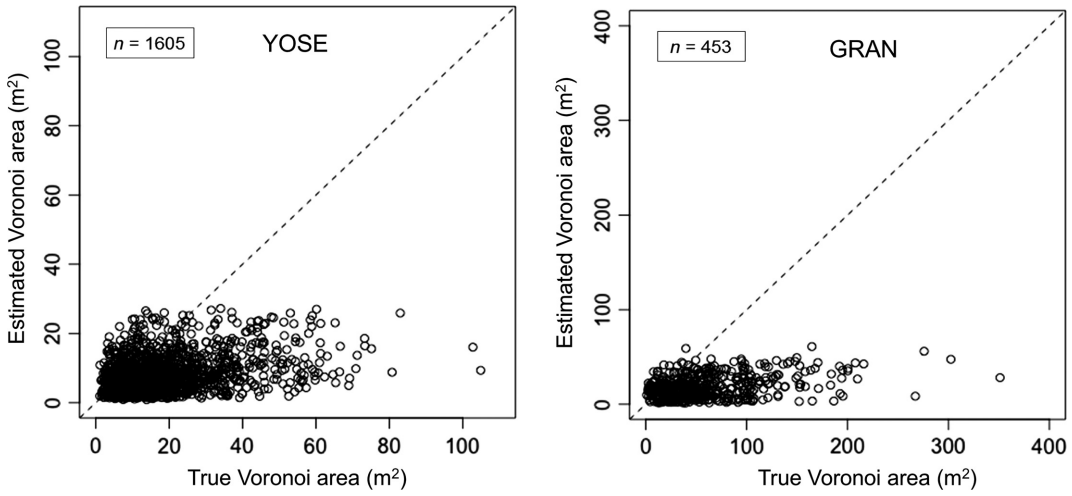


FIG. 5. The relationship between the true VA and the estimated VA (i.e., MVA) in the YOSE and GRAN sites. Estimated VA was calculated using the species-specific equation parameters provided in Baker (2014) and a MND estimated from a grid of 21 sampling points with four bearing trees at each point. Results for the other stands are shown in Appendix S1: Fig. S5.

Table S10). In contrast, Baker (2014) found strong relationships between MVA and CR with $r^2$ values ranging from 0.52 to 0.95 for these same conifer species. The weak predictive ability of CR in these mixed-conifer forests may be due to the fact that tree spacing can sometimes be more dependent on edaphic factors (Meyer et al. 2007) or disturbance legacies than on competitive interactions. On drier microsites or nutrient-poor soils or in old canopy gaps, some trees grow in relative isolation due to factors unrelated to competition or tree size. These circumstances occur across the semiarid Western U.S. forests in general (Larson and Churchill 2012) and specifically in the stands included in our analysis (e.g., Fig. 1; North et al. 2002, Fry et al. 2014). Only at our most dense site (PLUM, Table 2) where canopy approaches closure (canopy cover = 90%, Kayler et al. 2005) from the effects of 100 yr of fire suppression might spacing be influenced by crown area. Interestingly the least bias in the MHVD density estimate was observed at PLUM (RE = 1.16 for MHVD, 4 nn, 50 points, Table 3). Thus, it seems likely that the MHVD approach will overestimate tree density in the Sierra Nevada and in other forests of the arid Western United States with similar stand structure.

TABLE 4. The mean difference between the true VA and MVA (Eq. 7) for all trees ≥9.5 cm DBH, trees >20 cm DBH, and trees >60 cm DBH at each site.

| | True VA MVA ($m^2$) | | |
|---|---|---|---|
| Site | Trees ≥9.5 cm DBH | Trees >20 cm DBH | Trees >60 cm DBH |
| PLUM | 6.82 | 6.02 | 6.87 |
| YOSE | 10.1 | 9.61 | 14.4 |
| TEAK | 15.6 | 16.4 | 28.3 |
| META | 26.7 | 39.2 | 83.7 |
| BRID | 33.8 | 33.7 | 45.1 |
| GRAN | 43.6 | 45.7 | 71.2 |

*Notes:* Negative values indicate the extent to which the MVA underestimated the true VA. Sites are listed in order of decreasing stand density with PLUM being the most dense and GRAN the least dense.

Our critique of the MHVD does not extend to its underlying theory. Using the Voronoi area to measure the inclusion probability of the nearest tree in a PDE (Delince 1986) proved to be the best predictor of tree density in all simulations (Table 3; Appendix S1: Table S9). However, at the lower sampling intensities (i.e., <50 sampling points), the precision of the Delince PDE was low, resulting in large confidence intervals. This imprecision is not surprising given that the Delince PDE only considers the nearest tree to each point (1 nn) in its calculation (Table 1). The Delince PDE also had a tendency to underestimate the true tree density at the lower sampling intervals (Appendix S1: Fig. S2). Klein and Vilcko (2006) extend the VA-based PDE to include more than the nearest tree to each point in an effort to improve precision. Advances in tree mapping technology (e.g., laser hypsometers) make measuring the VA of trees in the field more efficient. Thus the VA-based PDEs are viable plotless methods for forest inventory. However, for GLO applications, the challenge of predicting VA with the available data severely limits its utility.

Our assessment of the MHVD as a theoretically sound but technically flawed means to reconstruct historical forest density from GLO data was constrained by the availability of data and the specificity of our question. The spatial scale of our analysis was on the order of hectares whereas the GLO data span square kilometers. As often noted (e.g., Engeman et al. 1994, Kronenfeld and Wang 2007, Bouldin 2008, Hanberry et al. 2011), the non-random dispersion of trees at the local level and

differences in tree density at the regional level affects PDE performance. Thus the stand-level tests presented here probably do not capture the full range of variation in forest structure present in the landscape sampled by GLO survey points, although we attempted to account for this by testing six stands of widely varying densities across >8° of latitude. We also restricted our focus to PDE performance under ideal conditions without complications from sampling inconsistencies or surveyor biases (sensu Bourdo 1956). Ongoing research in the Sierra Nevada and Sierra de San Pedro Martir (C. Restaino and H. Safford, *unpublished data*) seeks to address these constraints by testing PDEs at the landscape scale while also quantifying the influence of survey data quality.

The Morisita was consistently the least biased estimator of tree density from GLO data across a gradient of forest conditions (Appendix S1: Tables S1–S8). This result supports previous research that found the Morisita to be the best choice when bearing trees have an aggregated distribution. The Cottam (Bouldin 2008) and Pollard (Hanberry et al. 2011) tended to underestimate true density in these situations while the Morisita provided more accurate estimates. Note that we relied on the median as the measure of central tendency instead of the more commonly reported mean (e.g., Engeman et al. 1994, Hanberry et al. 2011). Given the right skew in the distribution of the simulations due to the fact that the minimum density was constrained at 0 while the maximum was unconstrained (i.e., zero-truncation), the median was less than or equal to the mean. Thus our conclusions regarding overestimates are based on a more conservative measure of central tendency. However, we also report the mean density from the simulations to allow comparison with previous efforts (Appendix S1: Tables S1–S9).

In our simulations, both the Morisita 4 nn and Morisita 2 nn predictors were unbiased in estimating density at a range of sampling intensities. Although the Morisita 4 nn was less biased and more precise than the 2 nn (e.g., Table 3), the Morisita 2 nn has the advantage of a larger potential sample intensity because both section and quarter corners can be included in the density estimate. Moreover, the Morisita 4 nn appears to be sensitive to local non-random dispersion (C. Cogbill, *personal observation*). The well-vetted performance of the Morisita 2 nn suggests it should be considered the current standard for GLO applications.

Pre-settlement forest conditions derived from the GLO records for the Sierra Nevada (Baker 2014) differ substantially from results based on inventories conducted before EuroAmerican influence and on reconstructions from live and dead plant material (Taylor 2004, North et al. 2007, Scholl and Taylor 2010, Collins et al. 2011, 2015, Barth et al. 2015, Stephens et al. 2015; Safford and Stevens 2017). Specifically, Baker (2014) rejected the prevailing hypothesis that the pre-settlement Sierra Nevada mixed-conifer forests were mostly open, park-like landscapes with low tree densities maintained by low to moderate severity fires. For example, in the vicinity of Yosemite National Park in the central Sierra Nevada, Collins et al. (2011) reported an average tree density of 52 trees/ha for trees ≥15.2 cm DBH in a 1911 timber inventory. Working in the same area, Scholl and Taylor's (2010) reconstruction of the 1899 forest put tree density at 86 trees/ha for trees ≥10 cm DBH. In the Yosemite Forest Dynamics Plot, a more mesic forest than Scholl and Taylor (2010), Barth et al. (2015) reconstructed forest density in 1900 to be between 62 and 122 trees/ha for trees ≥10 cm DBH. In contrast, the GLO estimate for the area including all of these direct density estimates (Table G1 in Baker 2014) was 212 trees/ha. The much greater tree densities obtained from the MHVD analysis of GLO data (Baker 2012, 2014) have been noted for forests in Oregon (Hagmann et al. 2013, 2014) and California (Collins et al. 2015, Stephens et al. 2015). Notably the magnitude of the differences, namely GLO densities two to five times larger than ones based on inventories or reconstructions, match the methodological bias detected in our analysis.

The management implications of these contrasting perspectives of the pre-settlement forest are significant. Baker (2014) used GLO-derived tree densities to infer that extensive stand-replacing fire was a major component in the natural disturbance regime of the Sierra Nevada mixed-conifer forests. This conclusion implies that ongoing efforts by forest managers to mitigate wildfire behavior (e.g., North et al. 2009, USFS 2011, 2013) are misguided. Subsequent papers have attempted to add support for this alternate interpretation about historical forest and fire interactions (Odion et al. 2014, Baker 2015), which collectively promote management practices that foster denser forests susceptible to high-severity fire. Although these authors posit other lines of evidence supporting this alternative perspective, the much higher estimates of tree density are the quantitative linchpin of the thesis (Baker 2014). The propensity of the MHVD to significantly overestimate tree density challenges the validity of the argument.

In this era of global change, historical conditions play an increasingly important role as we seek to inform the future by understanding the past (Safford et al. 2012). As forest conditions and disturbance impacts deviate from the range of natural variation (Safford and Stevens 2017), effective intervention depends on our knowledge of forest dynamics and our ability to explain the processes involved (Stephens et al. 2010). The GLO survey represents a spatially extensive window into the pre-settlement forest of the American West that complements the detailed site-specific information obtained from historical inventories and forest reconstructions. Given the paucity of data, there is a premium on methods that extract as much insight as possible. Innovation must be encouraged. At the same time, new methods must be independently validated, especially when they directly

impact management and policy. It is in this spirit of sound scientific practice that we present our findings.

Acknowledgments

This work was funded by the Baker-Bidwell Research Fellowship from the Department of Environmental Science, Policy, and Management at the University of California, Berkeley (C. R. Levine). We are grateful to the many field assistants who collected the mapped stand data at the six sites included in our study, and to three anonymous reviewers who provided feedback on this paper. Funding for the Yosemite Forest Dynamics Plot was provided by Utah State University, University of Washington, University of Montana, Washington State University, and the Smithsonian Institution ForestGEO. We thank the volunteers and staff who collected the data, who are individually acknowledged at http://yfdp.org. This paper was shared with W. Baker before submission. He provided information to the authors to correct inconsistencies in Williams and Baker (2011) and Baker (2014) that have not been published. We used this information in the development of this paper and thank him for providing it.

## Literature Cited

Aakala, T., S. Fraver, A. W. D'Amato, and B. J. Palik. 2013. Influence of competition and age on tree growth in structurally complex old-growth forests in northern Minnesota, USA. Forest Ecology and Management 308:128–135.

Baddeley, A., E. Rubak, and R. Turner. 2015. Spatial point patterns: methodology and applications with R. Chapman and Hall/CRC Press, London, UK.

Baker, W. L. 2012. Implications of spatially extensive historical data from surveys for restoring dry forests of Oregon's eastern Cascades. Ecosphere 3:1–39.

Baker, W. L. 2014. Historical forest structure and fire in Sierran mixed-conifer forests reconstructed from General Land Office survey data. Ecosphere 5:79.

Baker, W. L. 2015. Historical Northern spotted owl habitat and old-growth dry forests maintained by mixed-severity wildfires. Landscape Ecology 30:655–666.

Barth, M. A. F., A. J. Larson, and J. A. Lutz. 2015. Use of a forest reconstruction model to assess changes to Sierra Nevada mixed-conifer forest during the fire suppression era. Forest Ecology and Management 354:104–118.

Biging, G. S., and M. Dobbertin. 1992. A comparison of distance-dependent competition measures for height and basal area growth of individual conifer trees. Forest Science 38:695–720.

Biging, G. S., and M. Dobbertin. 1995. Evaluation of competition indices in individual tree growth models. Forest Science 41:360–377.

Bouldin, J. 2008. Some problems and solutions in density estimation from bearing tree data: a review and synthesis. Journal of Biogeography 35:2000–2011.

Bourdo, E. A. 1956. A review of the General Land Office survey and of its use in quantitative studies of former forests. Ecology 37:754–768.

Bragg, D. C. 2001. A local basal area adjustment for crown width prediction. Northern Journal of Applied Forestry 18:22–28.

Bytnerowicz, A., M. Fenn, S. McNulty, F. Yuan, A. Pourmokhtarian, C. Driscoll, and T. Meixner. 2013. Interactive effects of air pollution and climate change on forest ecosystems in the United States: current understanding and future scenarios. Pages 333–369 *in* R. Matyssek, N. Clarke, P. Cudlin, T. N. Mikkelsen, J.-P. Tuovinen, G. Wieser, and E. Paoletti, editors. Global dimension of air pollution as part of climate change. Elsevier, Amsterdam, The Netherlands.

Churchill, D. J., A. J. Larson, M. C. Dahlgreen, J. F. Franklin, P. F. Hessburg, and J. A. Lutz. 2013. Restoring forest resilience: from reference spatial patterns to silvicultural prescriptions and monitoring. Forest Ecology and Management 291:442–457.

Collins, B. M., R. G. Everett, and S. L. Stephens. 2011. Impacts of fire exclusion and recent managed fire on forest structure in old growth Sierra Nevada mixed-conifer forests. Ecosphere 2:UNSP 51.

Collins, B. M., J. M. Lydersen, R. G. Everett, D. L. Fry, and S. L. Stephens. 2015. Novel characterization of landscape-level variability in historical vegetation structure. Ecological Applications 25:1167–1174.

Cottam, G. 1949. The phytosociology of an oak woods in southwestern Wisconsin. Ecology 30:271–287.

Cottam, G., and J. T. Curtis. 1956. The use of distance measures in phytosociological sampling. Ecology 37:451–460.

Cressie, N. 2015. Statistics for spatial data, revised edition. John Wiley & Sons, New York, New York, USA.

Delince, J. 1986. Robust density estimation through distance measurements. Ecology 67:1576–1581.

Engeman, R. M., R. T. Sugihara, L. F. Pank, and W. E. Dusenberry. 1994. A comparison of plotless density estimators using Monte Carlo simulation. Ecology 75:1769–1779.

FIA. 2015. USFS Forest Inventory and Analysis National Program. Database version FIADB_1.6_0.0.02. https://www.fia.fs.fed.us/tools-data/

Fry, D. L., S. L. Stephens, B. M. Collins, M. P. North, E. Franco-Vizcaíno, and S. J. Gill. 2014. Contrasting spatial patterns in active-fire and fire-suppressed Mediterranean climate old-growth mixed conifer forests. PLoS ONE 9:e88985.

Fule, P. Z., T. W. Swetnam, P. M. Brown, D. A. Falk, D. L. Peterson, C. D. Allen, G. H. Aplet, M. A. Battaglia, D. Binkley, and C. Farris. 2014. Unsupported inferences of high-severity fire in historical dry forests of the western United States: response to Williams and Baker. Global Ecology and Biogeography 23:825–830.

Grimm, E. C. 1984. Fire and other factors controlling the Big Woods vegetation of Minnesota in the mid-nineteenth century. Ecological Monographs 54:291–311.

Hagmann, R. K., J. F. Franklin, and K. N. Johnson. 2013. Historical structure and composition of ponderosa pine and mixed-conifer forests in south-central Oregon. Forest Ecology and Management 304:492–504.

Hagmann, R. K., J. F. Franklin, and K. N. Johnson. 2014. Historical conditions in mixed-conifer forests on the eastern slopes of the northern Oregon Cascade Range, USA. Forest Ecology and Management 330:158–170.

Hanberry, B. B., S. Fraver, H. S. He, J. Yang, D. C. Dey, and B. J. Palik. 2011. Spatial pattern corrections and sample sizes for forest density estimates of historical tree surveys. Landscape Ecology 26:59–68.

Hanberry, B. B., B. J. Palik, and H. S. He. 2012. Comparison of historical and current forest surveys for detection of homogenization and mesophication of Minnesota forests. Landscape Ecology 27:1495–1512.

Hanson, C. T., and D. C. Odion. 2016. Historical forest conditions within the range of the pacific fisher and spotted owl in the Central and Southern Sierra Nevada, California, USA. Natural Areas Journal 36:8–19.

Hessburg, P. F., et al. 2015. Restoring fire-prone Inland Pacific landscapes: seven core principles. Landscape Ecology 30:1805–1835.

Hessburg, P. F., T. A. Spies, D. A. Perry, C. N. Skinner, A. H. Taylor, P. M. Brown, S. L. Stephens, A. J. Larson, D. J.

Churchill, and N. A. Povak. 2016. Tamm review: Management of mixed-severity fire regime forests in Oregon, Washington, and Northern California. Forest Ecology and Management 366:221–250.

Kayler, Z. E., L. B. Fortini, and J. J. Battles. 2005. Group selection edge effects on the vascular plant community of a Sierra Nevada old-growth forest. Madroño 52:262–266.

Klein, C., and F. Vilcko. 2006. Design-unbiased estimation for point-to-tree distance sampling. Canadian Journal of Forest Research 36:1407–1414.

Kronenfeld, B. J. 2009. A plotless density estimator based on the asymptotic limit of ordered distance estimation values. Forest Science 55:283–292.

Kronenfeld, B. J., and Y.-C. Wang. 2007. Accounting for surveyor inconsistency and bias in estimation of tree density from presettlement land survey records. Canadian Journal of Forest Research 37:2365–2379.

Larson, A. J., and D. Churchill. 2012. Tree spatial patterns in fire-frequent forests of western North America, including mechanisms of pattern formation and implications for designing fuel reduction and restoration treatments. Forest Ecology and Management 267:74–92.

Levine, C. R., F. Krivak-Tetley, N. S. van Doorn, J.-A. S. Ansley, and J. J. Battles. 2016. Long-term demographic trends in a fire-suppressed mixed-conifer forest. Canadian Journal of Forest Research 46:745–752.

Liu, F., D. J. Mladenoff, N. S. Keuler, and L. S. Moore. 2011. Broadscale variability in tree data of the historical Public Land Survey and its consequences for ecological studies. Ecological Monographs 81:259–275.

Lorimer, C. G. 1983. Tests of age-independent competition indices for individual trees in natural hardwood stands. Forest Ecology and Management 6:343–360.

Lutz, J. A., A. J. Larson, M. E. Swanson, and J. A. Freund. 2012. Ecological importance of large-diameter trees in a temperate mixed-conifer forest. PLoS ONE 7:e3613.

Mark, A. F., and A. E. Esler. 1970. An assessment of the point-centered quarter method of plotless sampling in some New Zealand forests. Proceedings of the New Zealand Ecological Society 17:106–110.

Mast, J. N., P. Z. Fule, M. M. Moore, W. W. Covington, and A. E. M. Waltz. 1999. Restoration of presettlement age structure of an Arizona ponderosa pine forest. Ecological Applications 9:228–239.

Maxwell, R. S., A. H. Taylor, C. N. Skinner, H. D. Safford, R. E. Isaacs, C. Airey, and A. B. Young. 2014. Landscape-scale modeling of reference period forest conditions and fire behavior on heavily logged lands. Ecosphere 5:1–28.

Meyer, M., M. North, A. Gray, and H. Zald. 2007. Influence of soil thickness on stand characteristics in a Sierra Nevada mixed-conifer forest. Plant and Soil 294:113–123.

Morisita, M. 1957. A new method for the estimation of density by spacing method applicable to nonrandomly distributed populations. Physiology and Ecology 7:134–144. English translation by USDA Division of Range Management 1960. http://math.hws.edu/~mitchell/Morisita1957.pdf

North, M., et al. 2002. Vegetation and ecological characteristics of mixed-conifer and red fir forests at the Teakettle Experimental Forest. General Technical Report PSW-GTR-186. USDA Forest Service, Pacific Southwest Research Station, Albany, California, USA.

North, M., J. Innes, and H. Zald. 2007. Comparison of thinning and prescribed fire restoration treatments to Sierran mixed-conifer historic conditions. Canadian Journal of Forest Research 37:331–342.

North, M., P. Stine, K. O'Hara, W. Zielinski, and S. Stephens. 2009. An Ecosystems Management Strategy for Sierra Mixed-Conifer Forests. General Technical Report PSW-GTR-220. USDA Forest Service, Pacific Southwest Research Station, Albany, California, USA.

Odion, D. C., C. T. Hanson, A. Arsenault, W. L. Baker, D. A. DellaSala, R. L. Hutto, W. Klenner, M. A. Moritz, R. L. Sherriff, and T. T. Veblen. 2014. Examining historical and current mixed-severity fire regimes in ponderosa pine and mixed-conifer forests of western North America. PLoS ONE 9:e87852.

Okabe, A., B. Boots, K. Sugihara, and S. N. Chiu. 2000. Concepts and applications of Voronoi diagrams. Second edition. John Wiley and Sons, Chichester, UK.

Perry, D. A., P. F. Hessburg, C. N. Skinner, T. A. Spies, S. L. Stephens, A. H. Taylor, J. F. Franklin, B. McComb, and G. Riegel. 2011. The ecology of mixed severity fire regimes in Washington, Oregon, and Northern California. Forest Ecology and Management 262:703–717.

Pollard, J. H. 1971. On distance estimators of density in randomly distributed forests. Biometrics 27:991–1002.

R Development Core Team. 2014. R: A language and environment for statistical computing. R Foundation for Statistical Computing, Vienna, Austria. http://www.R-project.org/

Rhemtulla, J. M., D. J. Mladenoff, and M. K. Clayton. 2009. Historical forest baselines reveal potential for continued carbon sequestration. Proceedings of the National Academy of Sciences USA 106:6082–6087.

Safford, H. D., and J. T. Stevens. 2017. Natural range of variation (NRV) for yellow pine and mixed conifer forests in the Sierra Nevada, southern Cascades, and Modoc and Inyo National Forests, California, USA. General Technical Report PSW-GTR-256. USDA Forest Service, Pacific Southwest Research Station, Albany, California, USA.

Safford, H. D., J. A. Wiens, and G. Hayward. 2012. The growing importance of the past in managing ecosystems of the future. Pages 319–327 *in* J. A. Wiens, G. Hayward, H. D. Safford, and C. M. Giffen, editors. Historical environmental variation in conservation and natural resource management. John Wiley and Sons, New York, New York, USA.

Scholl, A. E., and A. H. Taylor. 2010. Fire regimes, forest change, and self-organization in an old-growth mixed-conifer forest, Yosemite National Park, USA. Ecological Applications 20:362–380.

Schulte, L. A., and D. J. Mladenoff. 2001. The original US public land survey records: their use and limitations in reconstructing presettlement vegetation. Journal of Forestry 99:5–10.

Stephens, S. L. 2000. Mixed conifer and red fir forest structure and uses in 1899 from the central and northern Sierra Nevada, California. Madroño 47:43–52.

Stephens, S. L., and S. J. Gill. 2005. Forest structure and mortality in an old-growth Jeffrey pine-mixed conifer forest in north-western Mexico. Forest Ecology and Management 205:15–28.

Stephens, S. L., C. I. Millar, and B. M. Collins. 2010. Operational approaches to managing forests of the future in Mediterranean regions within a context of changing climates. Environmental Research Letters 5:024003.

Stephens, S. L., J. M. Lydersen, B. M. Collins, D. L. Fry, and M. D. Meyer. 2015. Historical and current landscape-scale ponderosa pine and mixed conifer forest structure in the Southern Sierra Nevada. Ecosphere 6:Article 79.

Stephens, S. L., B. M. Collins, E. Biber, and P. Z. Fule. 2016. U.S. federal fire and forest policy: emphasizing resilience in dry forests. Ecosphere 7:e01584.

Taylor, A. H. 2004. Identifying forest reference conditions on early cut-over lands, Lake Tahoe Basin, USA. Ecological Applications 14:1903–1920.

USFS. 2011. Region five ecological restoration: Leadership intent. March 2011. USDA Forest Service, Pacific Southwest Region, Albany, California, USA.

USFS. 2013. Ecological restoration implementation plan. R5-MB-249. USDA Forest Service, Pacific Southwest Region, Albany, California, USA.

Wiegand, T., and K. A. Moloney. 2004. Rings, circles, and null-models for point pattern analysis in ecology. Oikos 104:209–229.

Williams, M. A., and W. L. Baker. 2011. Testing the accuracy of new methods for reconstructing historical structure of forest landscapes using GLO survey data. Ecological Monographs 81:63–88.

Williams, M. A., and W. L. Baker. 2012. Spatially extensive reconstructions show variable-severity fire and heterogeneous structure in historical western United States dry forests. Global Ecology and Biogeography 21:1042–1052.

Williams, M. A., and W. L. Baker. 2014. High-severity fire corroborated in historical dry forests of the western United States: response to Fule et al. Global Ecology and Biogeography 23:831–835.

## Supporting Information

Additional supporting information may be found online at: http://onlinelibrary.wiley.com/doi/10.1002/eap.1543/full

## Data Availability

Data associated with this paper have been deposited in figshare https://dx.doi.org/10.6084/m9.figshare.4749892